JOURNAL OF MATERIALS SCIENCE 23 (1988) 488–496

Monitoring the early hydration mechanisms of hydraulic cement

W. J. McCARTER, A. B. AFSHAR*
Department of Civil Engineering, Heriot-Watt University, Edinburgh, UK

Cement is one of the most widely used construction materials with one billion tonnes used annually. From an engineering point of view, it is essential that cement sets and hardens in a correct manner, indeed, modification of the setting and hardening characteristics of cement by the use of admixtures is becoming widespread in the construction industry. The reaction between cement clinker and water is a complicated chemical process which results in a rigid matrix capable of sustaining load. The increase in strength of the cement matrix is the consequence of hydration and crystal formation within the paste. Understanding the mechanisms of hydration and how they can be modified could result in new cement blends and admixtures tailor-made to suit any particular set of design criteria. In this paper it is shown that the temporal change in electrical response can be used to monitor the progress of hydration, and give an insight into mechanisms of hydration. Data are presented for several cement paste consistencies over the frequency range 20 Hz to 300 kHz.

1. Introduction

The reaction between cement clinker† and water is an exothermic reaction which takes place in a number of stages. Traditionally, conduction calorimetry has been used to follow the sequence of hydration by monitoring the rate of heat liberation of the cement paste. A typical calorimetric curve for ordinary Portland cement is shown in Fig. 1, with the stages of hydration indicated I to IV.

The four stages in the hydration of cement paste (over the initial 24 h) can be summarized as:

(I) an initial period of rapid chemical activity and saturation of the gauging water with Ca^{2+} and OH^- ions, and other minor ions leached from the cement grains. Tricalcium silicate (C_3S) and tricalcium aluminate (C_3A) hydration predominate over this period;

(II) an induction, or dormant, period of apparent chemical inactivity and reduction in reaction rate;

(III) a period of renewed chemical activity, primarily on the C_3S phase, which results in an increase in internal temperature of the paste;

(IV) the beginning of the hardening period which is characterized by much slower reaction rates. Renewed activity on the C_3A phase can occur at the beginning of stage IV.

According to other investigators [1–4], peak 1 is the result of the first hydration products forming around the grain surfaces, primarily amorphous calcium-silicate-hydrates (C-S-H) on the C_3S phase and ettringite on the C_3A phase; peak 2 is due to the secondary hydration of C_3S forming more crystalline hydrates and precipitation of calcium hydroxide (CH). The shoulder in the curve at 3 is associated with C_3A reaction with large-scale formation of ettringite and monosulpho-aluminate and that occurring at 4 is the result of tetracalcium-alumino-ferrite (C_4AF) hydration.

Although heat of hydration methods relate hydration to the amount of heat evolved, the small sample size, together with the normally high water/cement ratios used in the test do not represent typical conditions occurring in practice. It should also be emphasized that in practice, concrete, hence cement, is mixed in large volumes. Moreover, because the heat-evolution curve represents a dynamic balance between the heat evolved by the hydrating paste to its surroundings, the exact shape and position of the peaks depend on the particular instrument used.

Setting and hardening of cement paste is the direct result of chemical reactions and phase transition occurring within the paste both on the grain surface and in the aqueous phase outwith the grain. Monitoring these chemical processes (rather than heat evolution which is a consequence of these reactions) would give a better insight into the understanding of the mechanisms of hydration and microstructural development within the paste.

2. Electrical response

When cement grains are added to water an exchange of ionic species initiates between the solids and the liquid phase. In such a system, charges will be electrostatically held onto the grain surface. The amount of charge and the strength by which they are held being dependent upon such factors as particle surface texture and net electrical charge on the particle itself.

**Present address*: A.M.A. Construction Ltd, 57 Dick Place, Edinburgh, UK.

†Ordinary Portland cement (OPC) comprises four main compounds which are written in shorthand form as: $C_3S = 3CaO \cdot SiO_2$, $C_2S = 2CaO \cdot SiO_2$, $C_3A = 3CaO \cdot Al_2O_3$, $C_4AF = 4CaO \cdot Al_2O_3 \cdot Fe_2O_3$.

0022–2461/88 $03.00 + .12

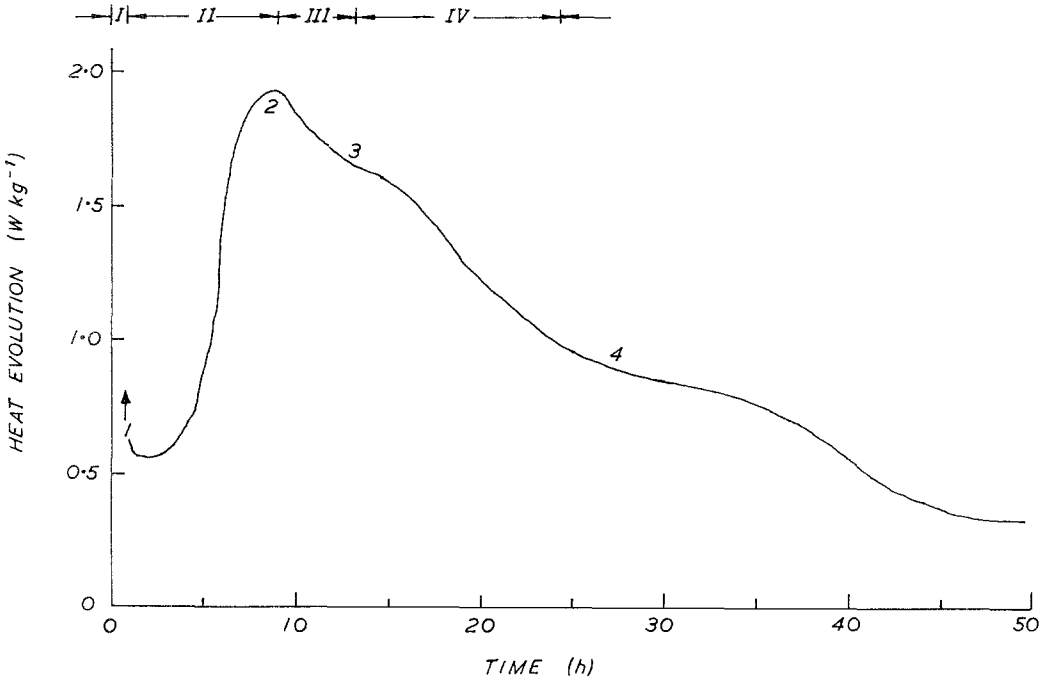

Figure 1 A typical conduction calorimetric curve for OPC.

The polarizability of these charges in an alternating electrical field will depend on, for example, types of charges, the degree of association of these charges with the particle surface, particle orientation and temperature of the system. Unbound charges in the aqueous phase will give rise to an ionic conduction effect on application of an electrical field. As the cement hydrates and the grains segment, the contribution to the electrical response from bound and unbound charges will change and will be reflected in the capacitance (hence, dielectric constant) and resistance (hence, resistivity) of the paste.

Much work has been undertaken on the electrical resistivity of cement paste in the hardened state [5–9] and during the initial (24 h) period of setting and hardening [10–13]. The prime motivation of this previous work has been to correlate the change in resistivity with physical characteristics of the paste (e.g. strength, setting time) and also in certain aspects of corrosion of steel in concrete. Little attention has been directed towards relating the change in resistivity to the mechanisms of hydration and chemical changes within the paste, although Tamas [14] has produced conductivity data on cement paste to this end. Detailed work on the variation of the dielectric constant is limited, as is the effect of frequency on both parameters, although some data are available [15–18] on the frequency effect over a limited range. The aims of this paper are (a) to present data on the electrical response of cement paste over an extended frequency spectrum, (b) to investigate if such response data can be used to identify the various stages of hydration as proposed from conduction calorimetry work, and (c) to investigate the mechanisms of hydration from the response data.

3. Experimental programme

3.1. Materials

Tests were undertaken using ordinary Portland cement (ASTM Type 1); the water/cement ratio was varied between 0.25 and 0.35 (by weight), a water/cement ratio of 0.27 producing a paste of standard consistency [19]. Distilled water was used and the cement was mixed using a planetary motion rotary mixer. Mixing time was kept constant at 2 min.

A chemical analysis of the cement is shown in Table I. A Bogue calculation of the main components is also given.

3.2. Data logging

The in-phase and quadrature of the impedance were measured at 28 spot frequencies over the range 20 Hz to 300 kHz using an impedance analyser (Wayne Kerr 6425); in addition, the internal temperature changes within the specimens were monitored using an HP3456A (Hewlett Packard Co. Ltd) digital voltmeter with compatible thermistor. The instruments were controlled and the data were logged, processed, and stored on floppy disc using an HP9836U microcomputer.

Experiments were run over a 24 h period with a reading cycle being initiated every 5 min. During each reading cycle the internal temperature of the

TABLE I Chemical analysis of OPC used in tests

Oxide composition (%)		Calculated compounds (%)	
SiO_2	20.47	C_3S	57.6
Al_2O_3	4.79	C_2S	15.3
Fe_2O_3	3.24	C_3A	7.2
CaO	64.42	C_4AF	9.8
MgO	2.61	$CaSO_4$	4.3
SO_3	2.54	Lime saturation factor	96.4
Na_2O	0.31		
K_2O	0.71		
Loss on ignition	1.0		
Insoluble residue	0.43		
Free CaO	1.2		

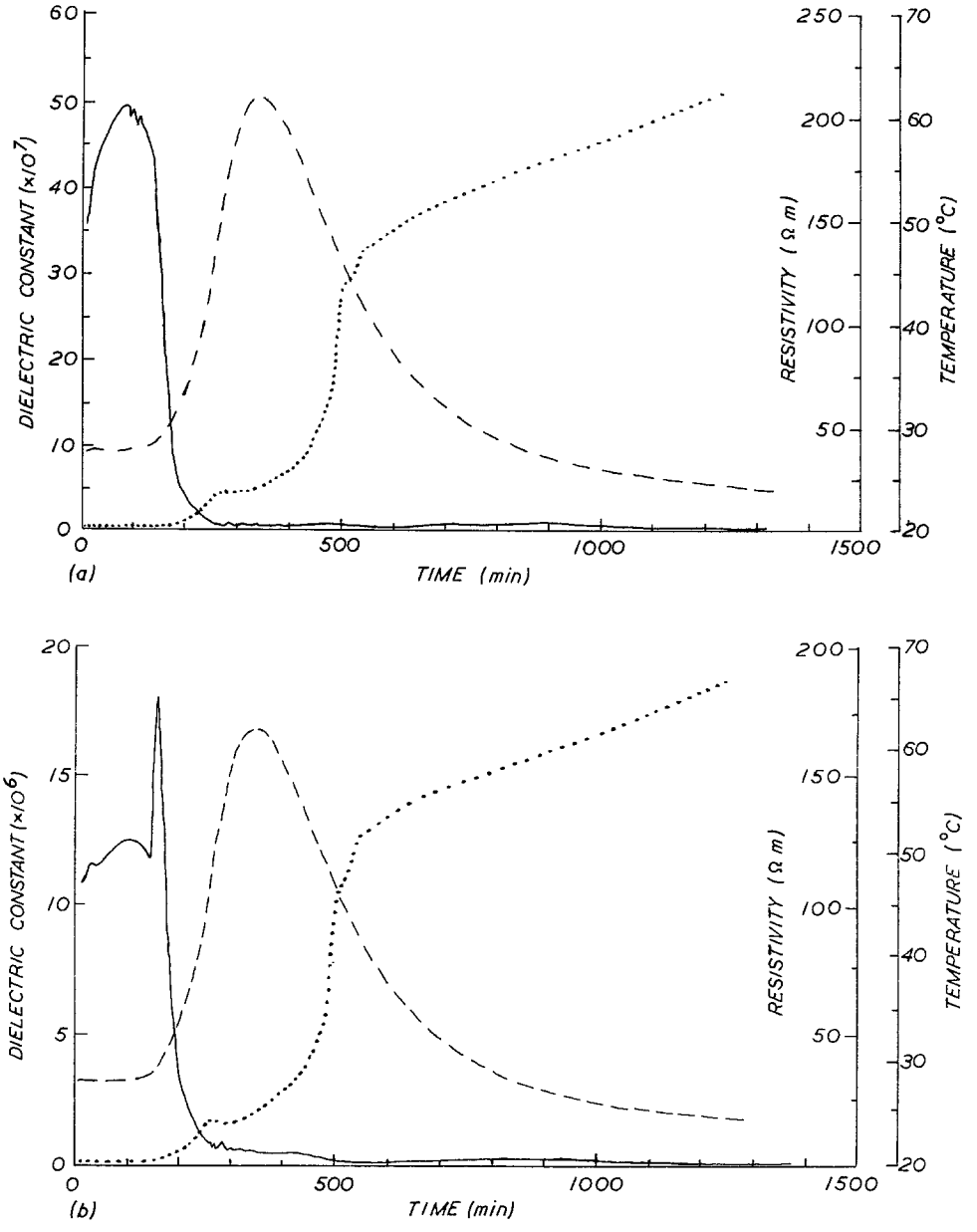

Figure 2 Variation of electrical parameters and internal temperature for OPC during initial 24 h. Frequency (a) 20 Hz, (b) 200 Hz, (c) 2 kHz, (d) 20 kHz, (e) 200 kHz. (——) Dielectric constant, (· · · ·) resistivity (– – –) temperature.

specimen was taken as was the capacitance (at 28 spot frequencies) and resistance (at 28 spot frequencies).

For each test, enough material was mixed to obtain two identical samples. One sample was used for electrical measurements and, in parallel, the other sample was used for internal temperature measurements. Both samples were placed in an environmental chamber to maintain constant ambient air conditions (25° C and 75% r.h.). For electrical measurements, the sample was contained in a dielectric cell and measurements were made using a four-terminal technique.

4. Discussion

Data are presented to show the variation in electrical response over the frequency range 20 Hz to 300 kHz during the initial 24 h after gauging. The results are typical of those taken from over 200 tests.

4.1. Variation of electrical parameters over initial 24 h

Fig. 2 displays the variation of dielectric constant and resistivity over five decades of frequency (20 Hz to 200 kHz) for a paste of water/cement ratio 0.27. The internal temperature change within the paste during hydration has been superimposed on the graphs for comparative purposes.

When water is added to cement grains, ions are rapidly leached from the grain surfaces (primarily Ca^{2+} and OH^-) leaving behind a surface layer rich in hydrosilicate ions (on the C_3S phase) giving the grain a net negative charge (Fig. 3a). Within a few minutes an amorphous, semi-permeable gel membrane of calcium-silicate-hydrate forms outside the surface layer, and, associated with the grain and gel, will be an electrical double layer (Fig. 3b). There is thus a physical barrier between the silica-rich surface layer and the diffuse double layer and bulk aqueous phase. This barrier will slow down reaction rates. Imbibation of water through the semi-permeable membrane results in continuous dissolution of the grains from within the Ca^{2+} and OH^- ions passing through the membrane (although many Ca^{2+} ions must remain within the negatively charged surface layer). The larger sterically hindered hydrosilicate ions remain within the gel

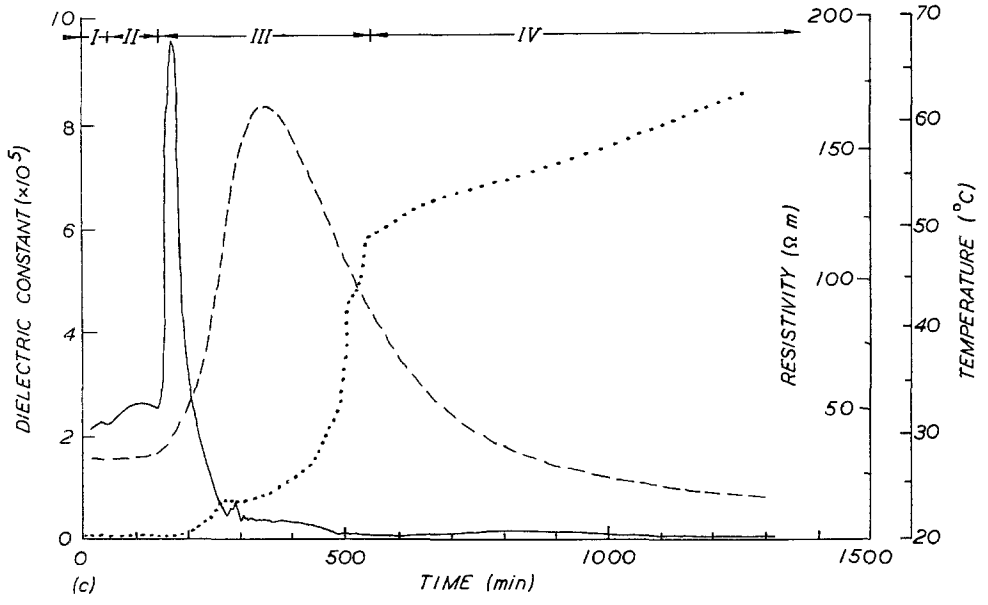

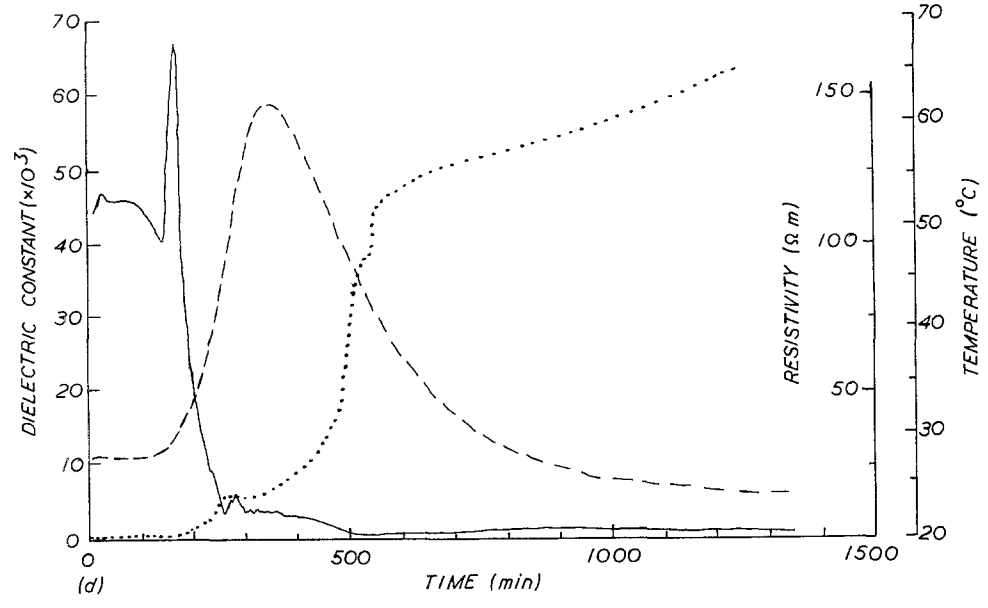

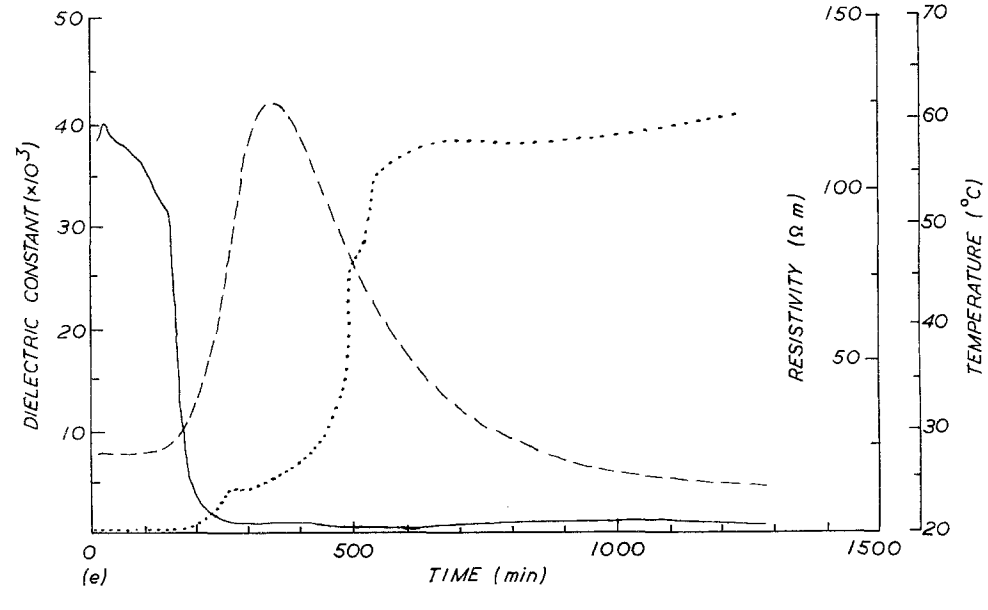

Figure 2 Continued

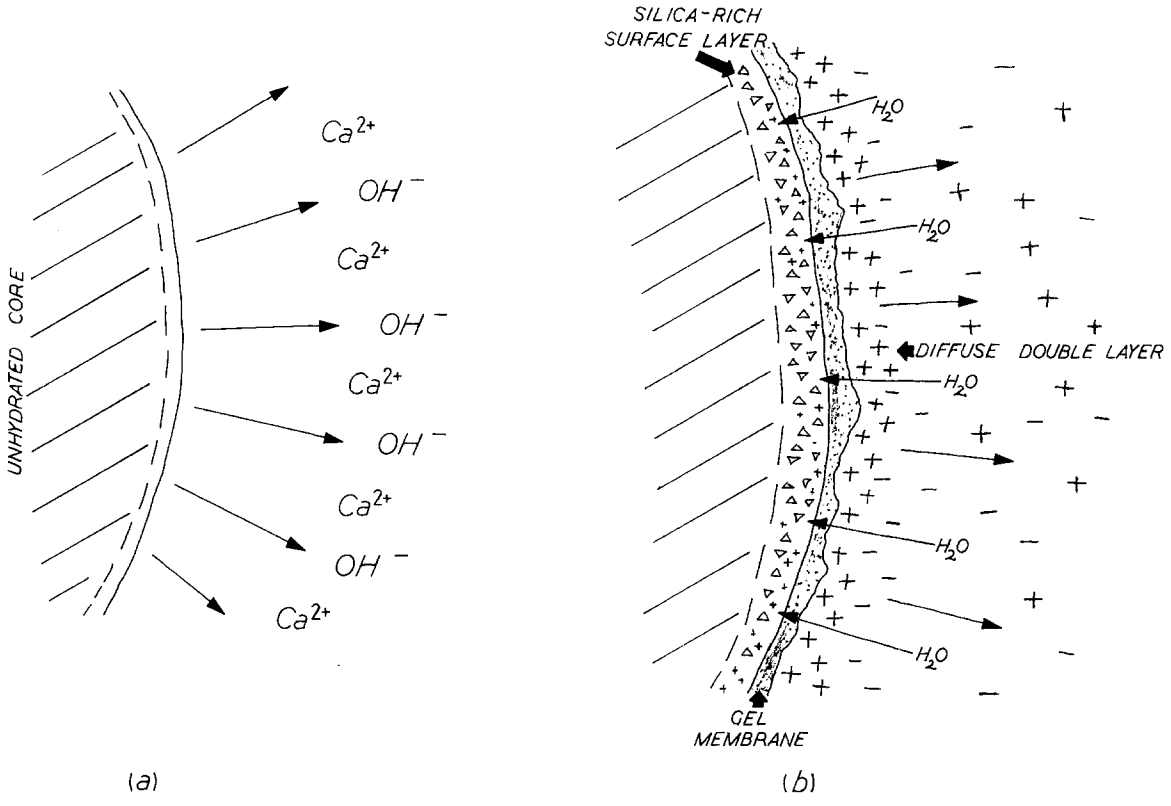

Figure 3 Schematic representation of cement grain during early hydrolysis and hydration, (a) immediately on gauging, (b) several minutes after gauging.

membrane. Thus, at the initial stages of hydration, there are varying degrees of charge mobility: (a) mobile unbound charges in the bulk aqueous phase, and (b) electrostatically bound charges of varying mobility in the diffuse double layer, gel and grain surface layer. Polarization of these surface charges can induce large dipole moments giving large dielectric constants [20, 21].

Considering the dielectric response curves shown in Fig. 2a to e, a general feature at any frequency is the variation of dielectric constant over the 24 h test period which decreases by more than two orders of magnitude. This, in broad terms, can be attributed to an irrotational binding of charges as the viscosity of the paste decreases. The resistivity curve also displays a marked change, and is a consequence of a reduction in ionic concentrations in the aqueous phase, and constriction of the continuous capillary pores due to grain segmentation and crystallization. Conduction paths thus become more tortuous as the paste increases in rigidity.

On gauging, the resistivity of the paste attains a relatively low value and continues to decrease during the initial 50 min (this feature is obscured by scale) and indicates that ions are passing into solution as the gel membrane builds up around the grain. The dielectric constant, on the other hand, increases as double layer charges and gel build-up on the grain and is more apparent as the frequency of applied field increases as at the higher frequencies only the more mobile charges can be polarized. Over the period 50 to 150 min, the resistivity increases only slightly (less than 10% of its initial value) indicating a slow build-up of gel and initial contact between grains. The dielectric constant displays a gradual variation over this period (50 to 150 min) and ends with a marked increase, reaching a maximum at 180 min. The prominence of this peak is dependent upon the frequency of the applied field and is observed over the range 80 Hz to 60 kHz. This is a result of the rupturing of the relatively weak gel membrane surrounding the grains caused by, (a) an increase in the osmotic pressure within the membrane [2], and, (b) the nucleation and growth of a calcium-silicate-hydrate "inner product" whose volume exceeds that of the dissolved anhydrous material.

The rupturing of the membrane allows water to reach the grains and results in accelerated dissolution of the grain and subsequent increase in polarizability of the paste. The renewed activity is associated with the grain and gel as the resistivity, which is related to ionic conduction through the continuous interstitial phase, shows no decrease at this point in time (180 min). Charges released through the ruptured surfaces quickly combine with those outside the gel to further precipitate C-S-H and calcium hydroxide.

Furthermore, the effect of the renewed exothermic activity is to increase the temperature within the paste as is highlighted by the temperature/time curve. There ensues a period of intense chemical activity and the consequences of the membrane rupture are, (a) grain segmentation, (b) an irrotational binding of charges due to crystallization of CSH and CH, and (c) constriction and blocking of the continuous capillary cavities.

In the early stages of hydration, the low-frequency resistivity of the paste will be dominated by ionic conduction processes and the measured resistance of the paste (see Fig. 4) can be expressed as

$$R = \frac{\varrho_p L_e}{A}$$

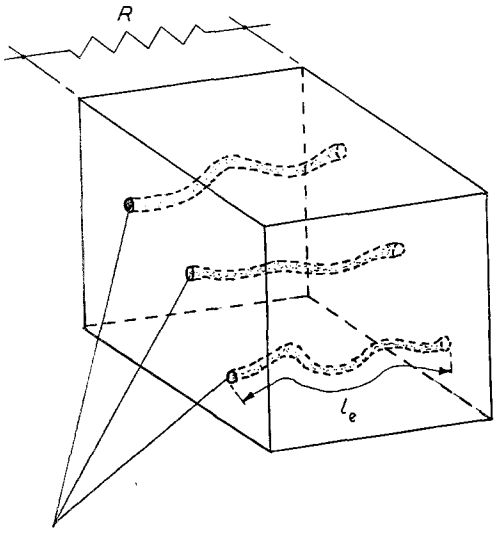

Figure 4 Simplified model for conduction through cement.

where ϱ_p is the resistivity of the pore fluid (Ωm) in the continuous water-filled capillaries, A is the total cross-sectional area (m^2) available for ionic conduction through the continuous capillaries, and L_e is the mean effective path length (m) of the continuous capillaries.

As the resistivity of the pore fluid will be sensitive to temperature changes ($\alpha \simeq 0.022\,^\circ C^{-1}$ [5, 9]), then, as the temperature of the paste increases the resistivity of the pore fluid will decrease. For the temperature rise within the samples (25 to 65° C) the resistivity of the pore fluid, hence the paste, would be expected to fall by almost 50%. However, at this point in time (250 to 450 min), the rigidity of the paste is increasing due to grain segmentation. The area, A, available for ionic conduction decreases and the continuous capillary paths become more tortuous as L_e increases. The result is an increase in the L_e/A ratio and, as is evident from the "plateau" region over this period, off-sets any drop in resistivity of the pore fluid. The influence of temperature rise within the paste on the electrical properties will thus depend on the rate of change of L_e/A.

The rate of change of resistivity considerably reduces after 600 min and, at the same time, the dielectric constant increases (although slightly obscured by scale). This feature is particularly noticeable at higher frequencies (Fig. 2e). This could signify further renewed activity within the paste resulting in a transient release of charges into the continuous and blocked capillary pores which will reduce the resistivity and increase the polarizability of the paste due to interfacial effects, respectively. Conversion of ettringite to monosulphoaluminate and renewed activity on the C_3A phase during which 2 mol Ca^{2+} and SO_4^{2-} are formed per 1 mol ettringite could be responsible for this feature. This would corroborate the work of Tamas [14] who obtained similar findings from conductivity data.

The authors have, for comparative purposes, identified the four stages of hydration from the electrical response data and are shown in Fig. 2c. The rate of change of the electrical parameters will be indicative of the rate of which reactions are progressing.

4.2. Dispersion and loss-angle curves over test period

The fall in dielectric constant with increasing frequency (dielectric dispersion) is shown in Fig. 5a, the dispersion curves being plotted at 10, 150, 300, 600 and 1200 min after gauging. Over the frequency range considered, a region of dispersion is apparent. As the paste increase in rigidity the polarizability of the paste decreases as charges become irrotationally bound and results in a displacement of the dispersion curves with time. One interesting feature is the dispersion curve plotted at 150 min (peak in dielectric constant) which shows an increase in polarizability of the paste above the initial curve (i.e. at 10 min) and a resulting increase in dielectric constant over the frequency range 80 Hz to 60 kHz. This is due to an increase in number of charges and/or an increase in charge mobility caused by the rupturing of the gel membrane surrounding the grain.

Fig. 5b displays the loss curve (tan δ) at 10, 150, 600 and 1200 min after gauging. The loss peak shifts from $\simeq$ 8 kHz at 10 min to $\simeq$ 12 kHz at 150 min after which it returns to $\simeq$ 6 kHz. In general, the loss angle decreases with time.

4.3. Effect of frequency on resistivity

Figs 6a to d shows the resistivity variation for a series of pastes made with water/cement ratios 0.25, 0.27, 0.30 and 0.35. The resistivity curves have been plotted for frequencies of 20 Hz and 300 kHz and the time at which the peak in dielectric constant occurs in the respective paste has been indicated (↓).

The resistivity of the paste remains relatively insensitive to frequency up to the time of peak in dielectric constant, thereafter the effect of increasing frequency is to reduce the resistivity of the paste. Several features are apparent from these curves: (i) as the water/cement ratio increases the absolute values of resistivity decrease, and is in agreement with previous studies, (ii) as the water/cement ratio increases the time at which the resistivity begins to rise (and peak in dielectric constant) is progressively delayed, (iii) the 20 Hz and 300 kHz resistivity curves for each paste begin to deviate noticeably after the peak in dielectric constant at which time the cement grains segment and the paste increases in rigidity. Regarding this latter point, if $\sigma_{d.c.}$ is the conductivity at d.c. (or low frequency) level and $\sigma_{a.c.}$ is the conductivity at a frequency above d.c. level then the frequency-dependent polarization conductivity can be represented by

$$\sigma'(\omega) = \sigma_{a.c.} - \sigma_{d.c.}$$

with the increase in conductivity due to surface ionic effects on the absorbed layer on the gel surface. The authors have quantified this effect in terms of resistivity by the introduction of a percentage frequency effect term (PFE) defined as

$$\text{PFE} = 100\,\frac{(\varrho_l - \varrho_h)}{\varrho_l}\,\%$$

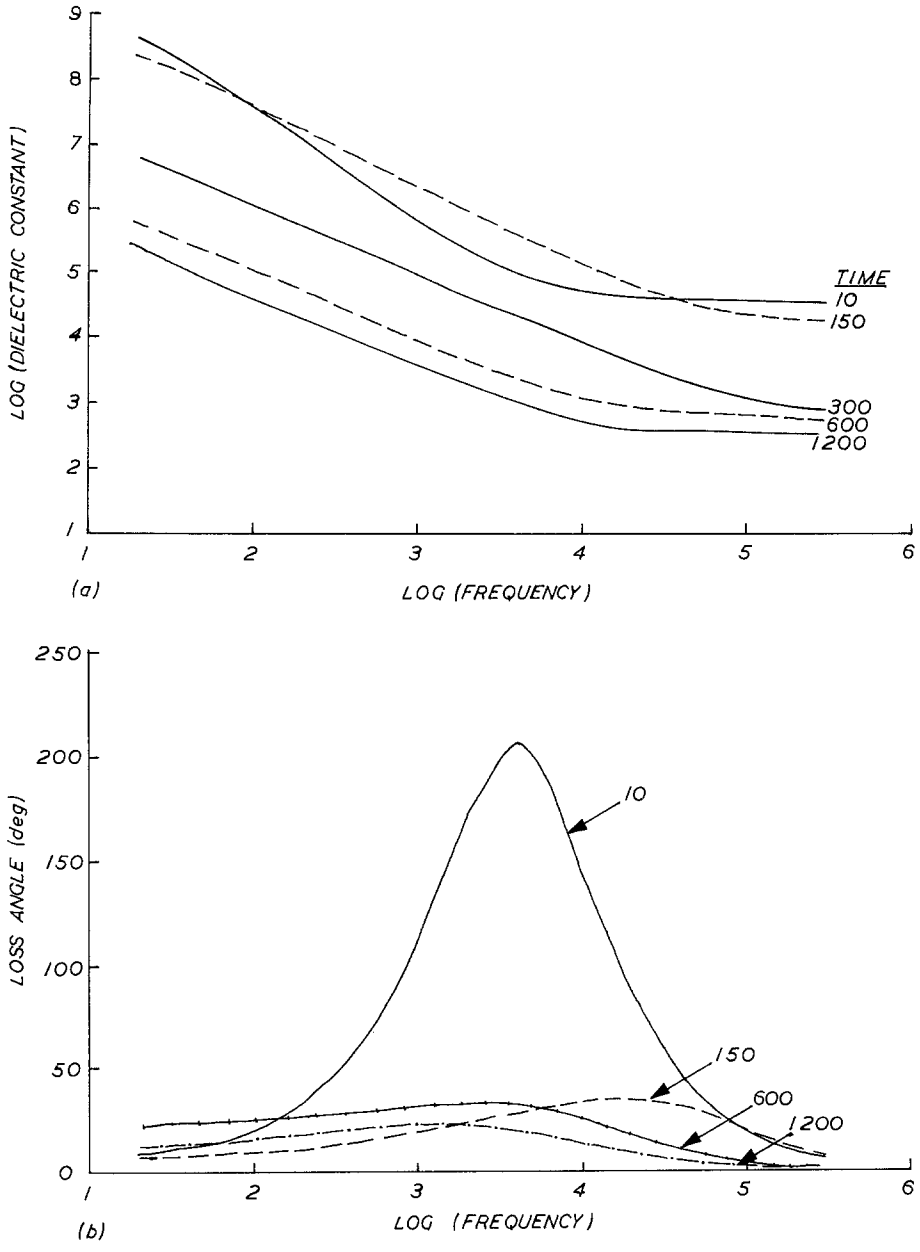

Figure 5 Dispersion and loss curves taken over the 24 h test period. (a) Dispersion curves, (b) loss curves.

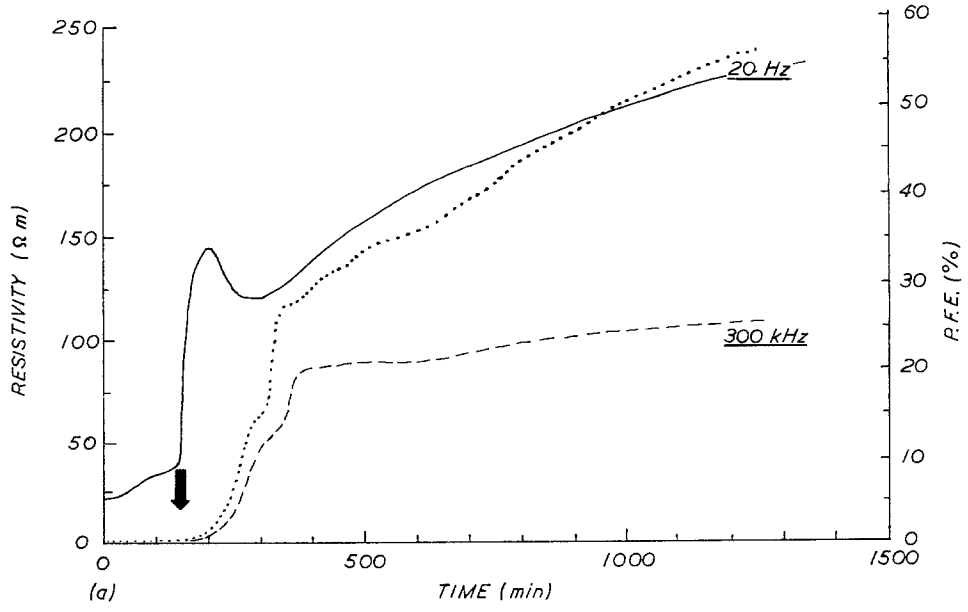

Figure 6 Effect of frequency of applied field on the electrical resistivity of the paste at four water/cement ratios (dotted and dashed lines represent resistivity values, the full line represents PFE). Water/cement ratio (a) 0.25, (b) 0.27, (c) 0.30, (d) 0.35.

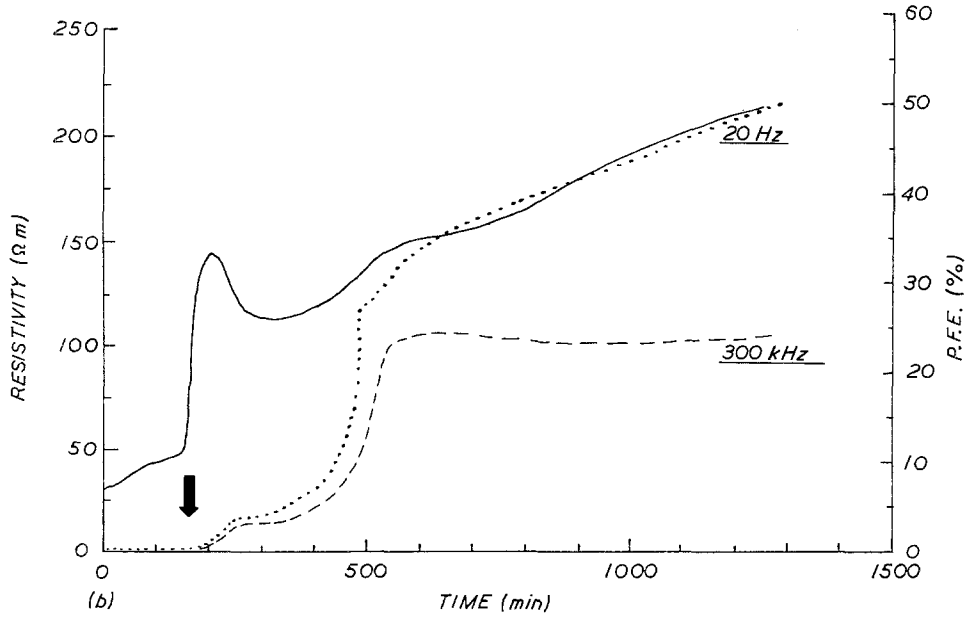

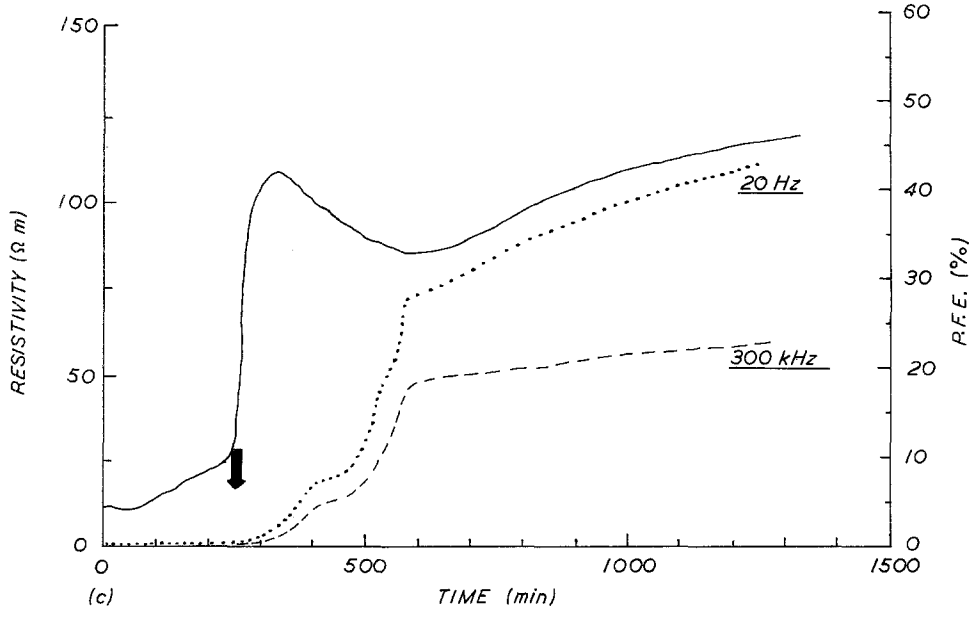

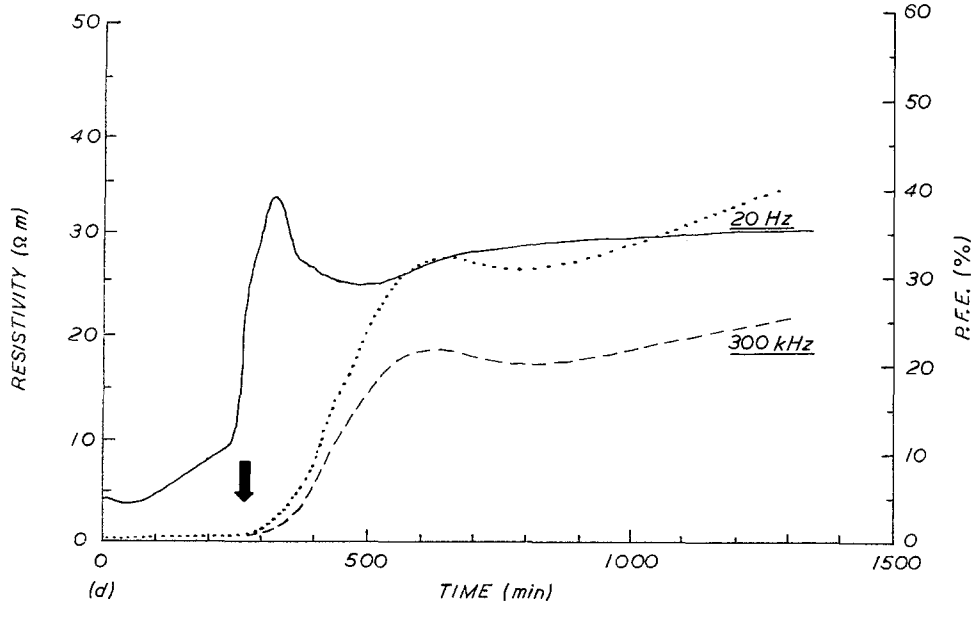

Figure 6 Continued

where ϱ_l is the resistivity at 20 Hz and ϱ_h is the resistivity at 300 kHz. This curve has been plotted in Figs 6a to d, which is plotted as the full line.

The PFE term increases with time, but the effect is more noticeable after grain segmentation and is apparent at all water/cement ratios. The frequency effect term could be visualized as a measure of the rate of constriction of the continuous capillary pores within the paste, as these pores become constricted due to crystal growth; the polarization conductivity, and hence frequency effect, increases. The smaller the diameter of the pores the greater the influence of the absorbed layer on the frequency effect term. A high-frequency effect would indicate a paste with small diameter pores hence a strong matrix and a low-frequency effect term would indicate a more open texture. Thus, as the water/cement ratio increases (and frequency effect decreases) the structure of the paste becomes more porous. This term could thus be used to give a measure of the permeability and rigidity of the paste.

5. Conclusions

The following conclusions can be drawn from the present study.

1. Data have been presented on the electrical properties of cement paste over the frequency range 20 Hz to 300 kHz and it has been shown that the dielectric constant and resistivity are not only functions of time but also frequency.

2. The electrical response of cement paste can be used to follow the sequence of hydration and give indications as to the mechanisms of hydration. Crystal growth and formation have a marked influence on the electrical properties of the paste and the electrical response of the paste could help in corroborating the various hydration theories, e.g. the osmotic membrane theory postulated by Birchall *et al.* [2].

3. Four stages of hydration have been identified over the initial 24 h. The rate of change of electrical parameters are indicative of the rate at which reactions are progressing.

In the hydration of cement, reactions at interfaces play a major role in determining the subsequent chemistry and strength development. Further development of electrical response measurements could offer an additional tool for investigating structure building mechanisms and microstructure development in cement paste. Such measurements could also be used as a fingerprint for cement hydration and linked to physical properties such as strength and permeability.

Acknowledgements

The authors wish to thank Professor A. D. Edwards for placing the facilities of his Department at their disposal. The receipt of a research grant (GR/D/38200) from the Science and Engineering Research Council is gratefully acknowledged. The authors are grateful to Clyde Cement Ltd, Coatbridge, Scotland for supplies of cement.

References

1. D. D. DOUBLE, A. HELLAWELL and S. PERRY, *Proc. R. Soc.* **A359** (1978) 435.
2. I. D. BIRCHALL, A. J. HOWARD and J. E. BAILEY, *ibid.* **A360** (1978) 445.
3. D. D. DOUBLE, *Phil. Trans. R. Soc.* **A310** (1983) 53.
4. P. L. PRATT and A. GHOSE, *ibid.* **A310** (1983) 93.
5. H. W. WHITTINGTON, W. J. McCARTER and M. C. FORD, *Mag. Concr. Res.* **33** (114) (1981) 48.
6. *Idem, Proc. Inst. Civ. Eng. (Lond.)* **2** (75) (1983) 123.
7. I. L. HANSSON and C. M. HANSSON, *Cem. Concr. Res.* **15** (1985) 201.
8. B. P. HUGHES, A. K. O. SOLEIT and R. W. BRIERLEY, *Mag. Concr. Res.* **37** (133) (1985) 243.
9. R. MORELLI, PhD thesis, University of Edinburgh (1985) p. 245.
10. K. E. DORSCH, *Cem. Concr. Manuf.* **6** (1933) 131.
11. J. CALLEJA, *J. Amer. Concr. Inst.* **23** (1952) 525.
12. R. SRIRAVINDRARAJAH and R. N. SWAMY, *Cem. Concr. Aggreg. (ASTM)* **4** (2) (1982) 73.
13. J. P. BARS, J. P. CAMPS and J. DEBUIGNE, *Mater. Struct. Res. Test.* **15** (85) (1982) 33.
14. F. D. TAMAS, *Cem. Concr. Res.* **12** (1982) 115.
15. W. J. McCARTER and A. B. AFSHAR, *J. Mater. Sci. Lett.* **3** (1984) 1083.
16. *Idem, ibid.* **4** (1985) 405.
17. *Idem, ibid.* **4** (1985) 851.
18. K. GORUR, M. K. SMIT and F. H. WITTMAN, *Cem. Concr. Res.* **12** (1982) 447.
19. British Standards Institution, BSI, London (1978) BS 4550, Part 3, Section 3.5.
20. H. P. SCHWAN, G. SCHWARZ, J. MACZUK and H. PAULY, *J. Phys. Chem.* **66** (1962) 2626.
21. G. SCHWARZ, *ibid.* **66** (1962) 2636.

Received 8 November 1986
and accepted 4 March 1987